COMPUTATIONAL COMPARISON BETWEEN TWO STENTING TECHNIQUES FOR THE LEFT MAIN CORONARY BIFURCATION

Politecnico di Milano

Laboratory of Biological Structure Mechanics

Dario Ardemani[1*], Francesco Bellavia[1*], Claudio Chiastra[1,2], Wei Wu[1], Julian Gunn[3], Francesco Migliavacca[1]

1. Laboratory of Biological Structure Mechanics (LaBS), Department of Chemistry, Materials and Chemical Engineering "Giulio Natta", Politecnico di Milano, Milan, Italy
2. Department of Cardiology, Biomedical Engineering, Erasmus MC, Rotterdam, The Netherlands
3. Department of Cardiology, Sheffield Teaching Hospitals, Sheffield, United Kingdom

*Authors equally contributed

Introduction

Percutaneous intervention through **stent deployment** of the **left main (LM) coronary bifurcation** has difficult clinical aspects. Currently, new stenting techniques are under investigation to improve clinical outcomes. In this study, numerical simulations are performed to compare the biomechanical influence of a standard technique (i.e. **simultaneous kissing stenting - SKS**) with a new one (i.e. **new simultaneous kissing stenting – NSKS**). A sequential numerical strategy is implemented. In particular, the deformed geometry of the artery, obtained from structural analysis of stent deployment, is used to extract the fluid domain for subsequent fluid dynamics simulations.

Materials and methods

Structural simulations

A three-layered hyperelastic idealized coronary bifurcation was created with an angle of 60° and internal diameters based on the mean values of a human LM (Fig. 1). Elastic angioplasty balloons were built to simulate the stent expansion. Stent geometries resembled the Resolute Integrity stent (Medtronic Inc., USA) with a cobalt-chromium alloy material.

The simulations of the SKS and NSKS stenting techniques (Fig. 2) were performed using **ABAQUS/explicit** (Dassault Systems Simulia Corp) as quasi-static processes.

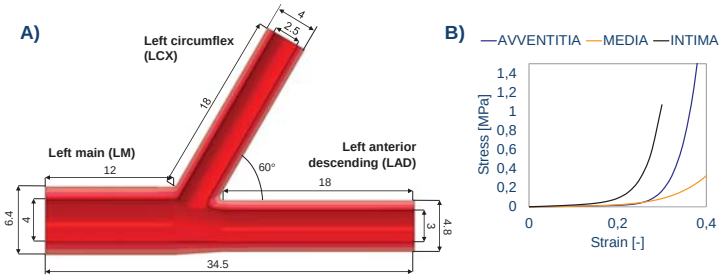

Fig.1 – A) 3D model of the left main coronary bifurcation. B) Mechanical behavior of the three arterial wall layers. All measures are in mm.

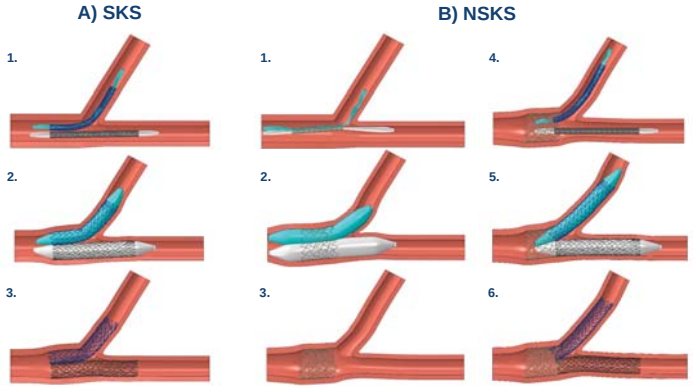

Fig.2 – A) Simulation steps of the SKS technique : 1) stents positioning; 2) expansion of the two stents; 3) final state after stent recoil. B) Simulation steps of the NSKS technique: 1) positioning of the first stent in the LM branch; 2) expansion of the stent in the LM branch; 3) final state for LM stenting; 4) positioning of two stents in the distal branches; 5) expansion of the stents in the distal branches; 6) final configuration after stent recoil.

Fluid dynamic simulations

The fluid domains were created starting from the final geometrical configurations of the structural simulations (Fig. 3a). A tetrahedral mesh was computed with a refinement of the elements at the stent struts and at stented bifurcation region (Fig. 3b). **Transient simulations** were carried out using **ANSYS Fluent** (ANSYS, Inc., USA). Physiological boundary conditions were applied at the inlet and the outlets (Fig. 4).

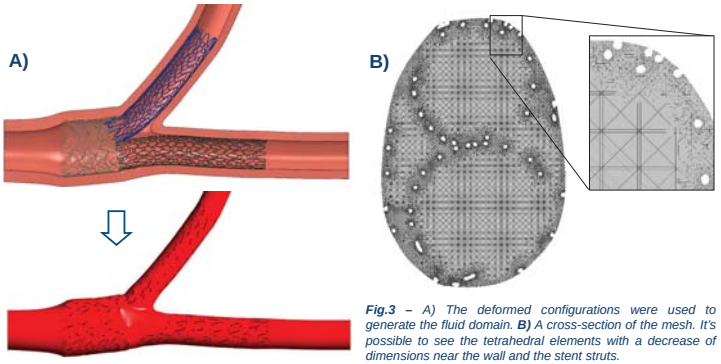

Fig.3 – A) The deformed configurations were used to generate the fluid domain. B) A cross-section of the mesh. It's possible to see the tetrahedral elements with a decrease of dimensions near the wall and the stent struts.

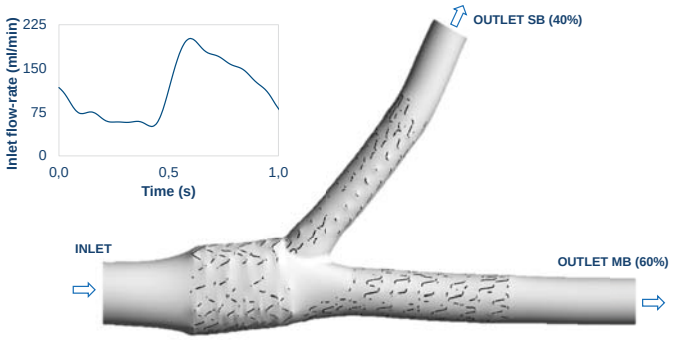

Fig.4 – Boundary conditions for transient simulations. At the inlet a pulsatile flow with flat velocity profile [1] was applied. At the outlets a flow split was imposed [2].

Results

Structural simulations

Geometrical configurations after stenting with SKS and NSKS techniques were compared by evaluating the position of the stent struts and the wall stress. In particular, **malapposition** (i.e. struts not in contact with the lumen surface) was higher in SKS than NSKS (Fig. 5), due to the long metallic carina in the LM branch. The evaluation of the **wall stress** gave a measure of the damage on the inner surface of bifurcation. Contour maps of maximum principal stress after stent recoil showed that the area with high stress was higher in the NSKS then SKS (Fig. 6), due to the overexpansion of the proximal main branch stent.

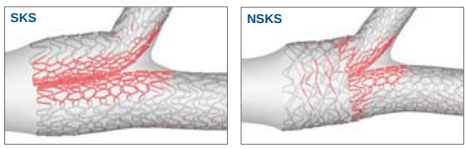

$malapp^{SKS} = 33\%\ vs.\ malapp^{NSKS} = 18\%$

Fig.5 – Malapposition in the SKS (left) and NSKS (right). Malapposed struts are highlighted in red.

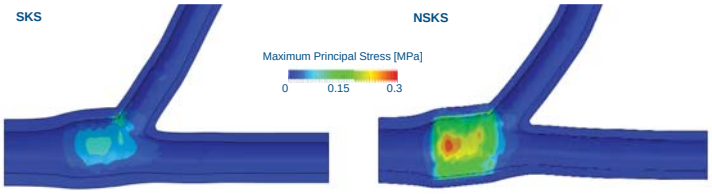

Fig.6 – Contour maps of maximum principal stress on the inner wall of the bifurcation for SKS (left) and NSKS (right).

Fluid dynamic simulations

The presence of a **long metallic carina** in the SKS model caused flow separation in the proximal main branch with the creation of two inner channels with an increase of the flow velocity (Fig. 7-left). **Recirculation regions** are also present in the SKS model. In both cases there blood **stagnation areas** were located near metallic struts. In particular, in NSKS model the LM stent caused a wider stagnation region close to the LM wall (Fig. 7b). Hemodynamic forces on the inner surface of the bifurcations were evaluated by calculating time-averaged **wall shear stress** (TAWSS). Results showed a larger area with low TAWSS in NSKS than SKS (Fig. 8), which is caused by the presence of fewer malapposed struts (especially in the LM branch).

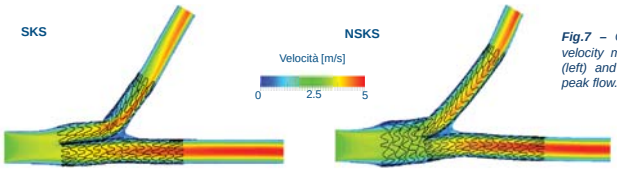

Fig.7 – Contour maps of velocity magnitude in SKS (left) and NSKS (right) at peak flow.

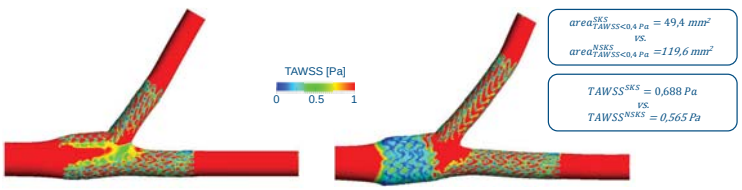

Fig.8 – Contour maps of TAWSS for SKS (left) and NSKS (right).

Conclusions

In this study, structural and fluid dynamic models were implemented to compare two different stenting techniques in an idealized model of the LM bifurcation. NSKS resulted in better outcomes in terms of malapposition than SKS, with a better coverage of each branches. This aspect induced a better velocity distribution, smaller blood stagnation areas and no blood recirculation. The main disadvantages of the NSKS were the larger area with higher wall stress and the larger area with low TAWSS at the lumen surface.

Contact: **claudio.chiastra@polimi.it**

References:
[1] Davies et al. 2006. Circulation, 133: 1768-1778; [2] Van der Giessen et al. 2011. J. Biomech, 44,6: 1089-1095